

# Thalamic features extraction and analysis in magnetic resonance imaging of preterm infants

Emiliano Trimarco<sup>1,\*†</sup>, Bahram Jafrasteh<sup>1,†</sup>, Simón Pedro Lubiañ-López<sup>2,3</sup> and Isabel Benavente-Fernández<sup>1,2,3</sup>

<sup>1</sup>Biomedical Research and Innovation Institute of Cádiz (INIBICA) Research Unit, Puerta del Mar University, Cádiz, Spain

<sup>2</sup>Division of Neonatology, Department of Paediatrics, Puerta del Mar University Hospital, Cádiz, Spain

<sup>3</sup>Area of Paediatrics, Department of Child and Mother Health and Radiology, Medical School, University of Cádiz, Cádiz, Spain

## Abstract

Preterm birth is the primary cause of infant death and is associated with later neurodevelopmental impairments. Neuroimaging is a powerful tool to analyse neuroanatomy abnormalities in preterm infants. It allows analysing of different brain structures, such as the thalamus and their alterations. Thalamus is a crucial hub for regulating cortical connectivity. Moreover, white matter (WM) injury in preterm infants can impact thalamic growth and maturation in long-term periods. Therefore, the study of the thalamus morphology during the neonatal period using magnetic resonance imaging (MRI) can help to identify those features that predict neurodevelopmental outcomes in these vulnerable population. In this study, we automatically segmented the thalamus structure from 3D MRI scans and extracted the thalamic features from these segmentations. The gestational age at birth and post-menstrual age at the scan time is also taken into account in our study. The K-means clustering, an unsupervised machine learning algorithm, was employed to explore the hidden pattern related to thalamus features from early and term-equivalent scans. Finally, we studied the association of these features to a scoring system used in clinical settings to assess MRI scans in very preterm infants at term-equivalent age. The main results highlight that 77 percent of preterm-born infants with abnormal MRI scores share the same cluster.

## Keywords

Thalamus, K-means clustering, Atlas-based segmentation, Preterm infants

## 1. Introduction

Preterm birth, before 37 weeks of gestation, affects fifteen million children each year in the world [1]. It remains the main cause of infant death [1]. The severity of long-term neurodevelopmental impairments increases with decreasing gestational age [2]. In particular, early exposure to extrauterine life is closely associated with deficits in cognitive, motor, visual, socio-emotional, sleep, and language domains [3]. The thalamus is a meaningful hub that shapes brain connectivity during prenatal and postnatal life. It is commonly affected in preterm infants by white

---

DETERMINED 2022: Neurodevelopmental Impairments in Preterm Children – Computational Advancements, August 26, 2022, Ljubljana, Slovenia

\*Corresponding author.

†These authors contributed equally.

✉ emiliano.trimarco@inibica.es (E. Trimarco); jafrasteh.bahram@uca.es (B. Jafrasteh); simonp.lubian.sspa@juntadeandalucia.es (S. P. Lubiañ-López); isabel.benavente@uca.es (I. Benavente-Fernández)



© 2022 Copyright for this paper by its authors. Use permitted under Creative Commons License Attribution 4.0 International (CC BY 4.0).

CEUR Workshop Proceedings (CEUR-WS.org)

matter (WM) injuries, either directly or through maturational disruption [4, 5]. Preterm birth influences the growth of thalamocortical connectivity and the steps in the sensory organisation and functional specialisation of the cerebral cortex [6, 7]. Thalamo-cortical connectivity is regionally altered for preterm infants, and the thalamic volume is related to both the cortical volume and the WM tracts [8]. There is also some evidence that alterations in fronto-temporal and parieto-occipital cortical areas are related to the thalamic structural connectivity, and the volumetric measurements obtained from the thalamic region [9]. Thalamocortical connectivity abnormalities identified after preterm birth can be correlated with the future neurodevelopmental impairments [10, 11, 12].

In this study, we develop a protocol to evaluate the importance of thalamic features of preterm infants. Our hypothesis aims to relate the morphological characteristics of the thalamus to the Kidokoro score [13]. Firstly, we use an automatic method to segment Magnetic Resonance Images (MRIs) from a preterm infant cohort [14]. Then, we extract morphological features from the region of interest (ROI), i.e. the segmented thalamus area. After an exploratory analysis of the extracted features, an unsupervised machine learning algorithm is used to cluster the features. Finally, we show that it is possible to cluster the abnormal MRIs through thalamus measurements using term-equivalent scans. In addition, the results show the extracted features are sufficient to differentiate between healthy term-born infants and preterm infants at term-equivalent age.

## 2. Method

### 2.1. Atlas correction and automatic thalamus segmentation

Melbourne Children’s Regional Infant Brain (M-CRIB 2.0) atlas [15] is used to segment thalamus structure from the MRI images of our cohort. In particular, the atlas contains ten scans from healthy term-born infants [15].

Preliminary visualization of the M-CRIB 2.0 atlas showed an overestimation of thalamic segmentation, including the nuclei and the hippocampal gyrus. Therefore, an expert in our group reviewed and corrected thalamic segmentation manually. We automatically segmented the thalamus from the MRI images according to the neonatal pipeline proposed by Makropoulos et al. [14, 16]. In principle, the pipeline registers the image to a neonatal atlas image at a similar gestational age [16] to separate non-cortical grey matter from the WM, grey matter and the cerebrospinal fluid (CSF). Then, the image is registered to the M-CRIB 2.0 atlas. Finally, local atlas weighting and DrawEM [16] are used to separate the thalamus from the other brain structures. This pipeline is widely used and supported by the literature studies [17, 18]. According to the changes made in the atlas, we adapted the pipeline [14] for thalamus segmentation. The clinical experts in the group have verified the quality of the automatic segmentation.

Figure 1(a)-1(c) shows an example of the original scan from the atlas, a corrected scan with a redundant part, and one of the segmentation provided by the pipeline after the correction, respectively.

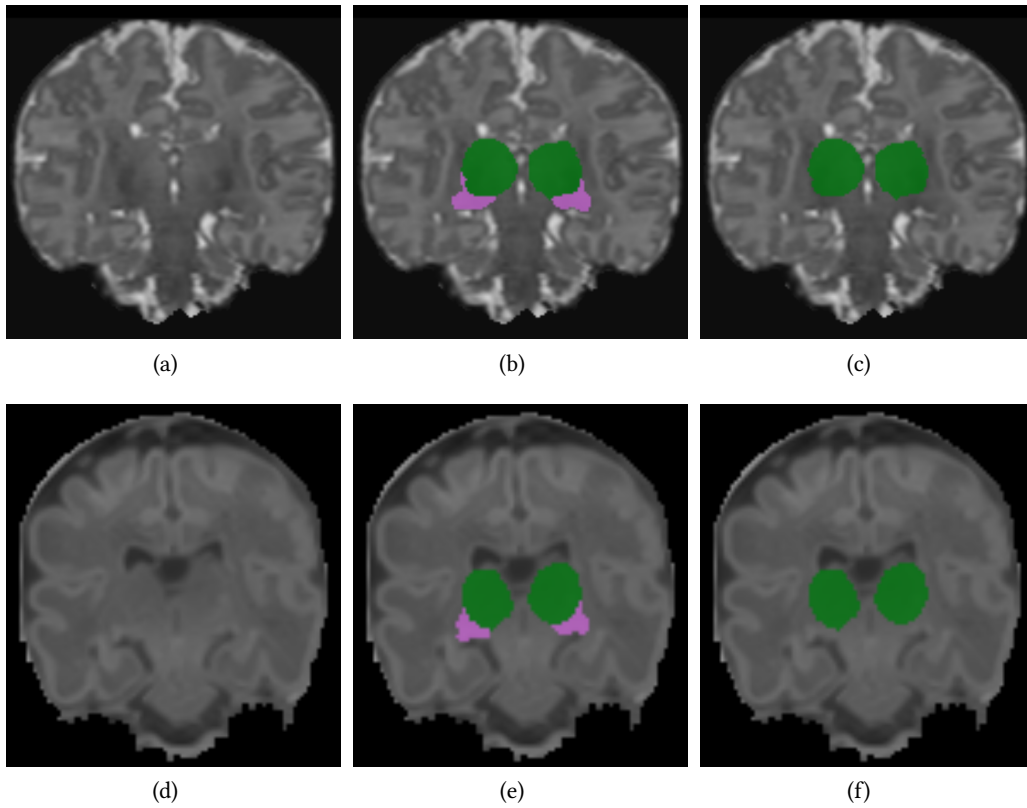


**Figure 1:** Atlas correction and the segmentation results. a) A slice from the coronal plane of the original atlas T2. b) A slice from the coronal plane of the correction in the atlas. c) A slice from the coronal plane of the corrected thalamus segmentation in the atlas. d) A slice from the coronal T1 plane of the preterm infant at term-equivalent age. e) A slice from the coronal plane of the automated segmentation in preterm infants at term-equivalent age. f) A slice from the coronal plane of segmented thalamus in preterm infants at term-equivalent age. The green colour indicates thalamus structure, and the purple colour refers to the corrections made by an expert on the atlas.

## 2.2. Thalamic feature extraction

We extracted ten features from the segmented thalamus (Table 2). All the volumetric measurements have been standardised by the Total Brain Volume (TBV). We prioritise TBV over Intra-Cranial Volume (ICV) as ICV includes extra-axial CSF. A physiological increase in extra-axial CSF in preterm infants may facilitate suboptimal brain growth in the neonatal period. Therefore, it is crucial to prioritise the TBV over the ICV to ensure measuring real brain tissue. The other measurements, like area, have been standardised by the maximum brain area at the axial plane, where the thalamus has the largest area. The following thalamus features are summarised in Figure 2 and Table 1: post-menstrual age (PMA) at the scan time, the TBV, the Standardised Left Thalamus 3D Surface (SLTS) and the Standardised Right Thalamus 3D Surface (SRTS). Furthermore, the other extracted variables are reported in Table 2. Notably, the 3D surface of the thalamus is standardised by the largest area of the brain in the axial plane. In

this way, we obtain an indirect measurement regarding the relationship between the thalamus and general brain maturation. The distributions of the four variables are shown in the diagonal boxes of Figure 2 and in Table 1. Moreover, Figure 2 shows the two-way relationships between these variables. For example, the last row of Figure 2 reveals that the volume brain increases with increasing PMA, but the standardised 3D surface of the thalamus decreases with increasing PMA. Since the brain regions grow considerably during this period, this behaviour is seen in this figure [19], and their proportion to the thalamus changes. Therefore, it affects the data standardisation and a value decrease does not concur with a natural reduction. It is relative to the growing trend of the TBV.

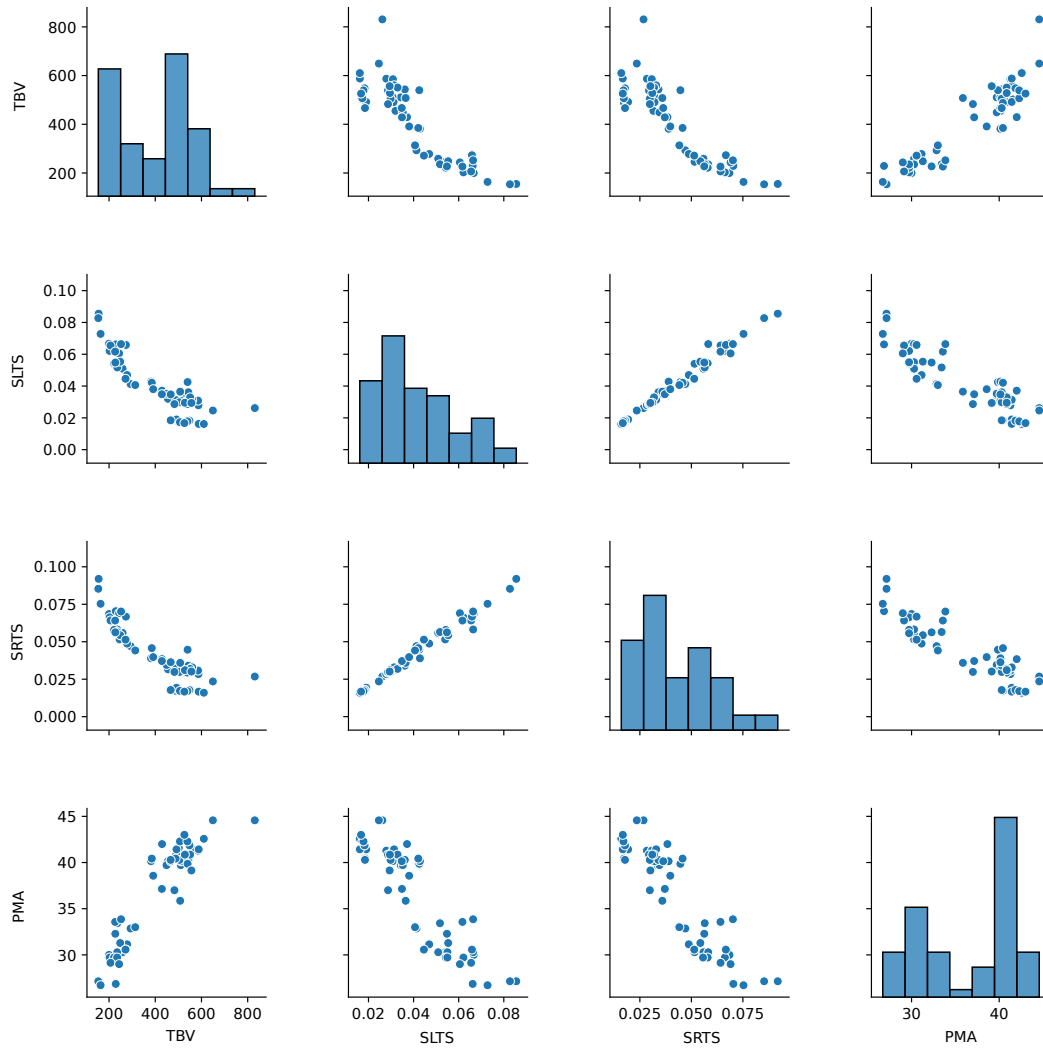


**Figure 2:** Distribution of Total Brain Volume in  $\text{cm}^3$  (TBV), Standardised Left Thalamus 3D Surface (SLTS) and Standardised Right Thalamus 3D Surface (SRTS), post-menstrual age in weeks (PMA) in the diagonal boxes and the two-way relationships in the other boxes

**Table 1**

Statistical description of Total Brain Volume (TBV), Standardised Left Thalamus 3D Surface (SLTS) and Standardised Right Thalamus 3D Surface (SRTS), post-menstrual age (PMA)

	TBV (cm <sup>3</sup> )	SLTS	SRTS	PMA (weeks)
Mean	402.37	0.041	0.042	36.494
S.D.	156.47	0.018	0.019	5.462
Min	153.60	0.016	0.016	26.715
25%	244.80	0.029	0.030	30.571
50%	448.93	0.036	0.037	39.715
75%	527.14	0.055	0.056	40.857
Max	830.73	0.086	0.092	44.571

### 2.3. MRI Score

MRI scans were acquired using a 1.5 Tesla scanner (Magnetom Symphony, Siemens Health Care, Erlangen, Germany) located in the radiology unit in the University Hospital of Puerta del Mar (HUPM), Cadiz, Spain. The acquisition parameters are as follows: spacing in x, y and z direction : 0.8, 0.8, 0.8; echo time = 3.67 ms; flip angle = 15° and repetition time = 1910.0 ms. T1 weighted spin echo imaged sequences were used to collect our data. Potential risks caused by the physical properties of the MRI equipment were evaluated and minimised following the recommendations provided for preterm infants [20] and our previous experiences [21, 22]. The images obtained from the scans were evaluated through the clinicians' observation using a scoring system developed by Kidokoro et al. [13]. It provides a comprehensive and objective characterisation of the regional and global brain lesions and brain growth. In particular, it is used to confirm the clustering results and check whether patients with an abnormal score are clustered into the same group (For more details, see section 4.2). The scoring system suggested by Kidokoro et al. [13] groups the global score into four categories: (normal, mild, moderate, and severe). We then binarised the variable by considering normal versus abnormal MRI (the latter including mild, moderate and severe) as we wanted to see if the thalamic features could be associated with any degree of MRI abnormality.

### 2.4. K-means clustering

Given a set of observations having  $D$  dimensions, the k-means clustering as an unsupervised machine learning algorithm aims to partition the observations into  $k$  different groups by minimising within cluster sum of the squared error without having access to the outcomes. We set  $K$  to three in our analysis because our dataset has three main groups (see section 3). It should be noted that clustering is only carried out based on the thalamic features. Table 2 shows the included attributes for K-means clustering. The K-means clustering is also performed using morphological features extracted from the atlas images. Moreover, the score proposed in Kidokoro et al. [13] was used to validate the K-means algorithm. In conclusion, according to the preliminary statistical analysis, the plots of each feature vs others (Figure 4), and other algorithms comparison, we conclude that K-means clustering as a simple algorithm can efficiently cluster our dataset (table 4).

**Table 2**

List of dataset variables included in the clustering. Total Brain Volume (TBV), Standardised Left Thalamus 3D Surface (SLTS), Standardised Right Thalamus 3D Surface (SRTS), post-menstrual age (PMA)

Variable	Clustering
TBV (cm <sup>3</sup> )	included
Left Thalamus Volume (cm <sup>3</sup> )	included
SLTS	included
Left Thalamus perimeter (cm)	included
Left Thalamus Angle (degrees)	included
Right Thalamus Volume (cm <sup>3</sup> )	included
SRTS	included
Right Thalamus perimeter (cm)	included
Right Thalamus Angle (degrees)	included
Distance Left and Right Thalamus cm	included
Angle between Left and Right Thalamus	included
Left Centroid	not included
Left Highest Point	not included
Right Centroid	not included
Right Highest Point	not included
Kidokoro score	not included
SEX	not included
GA	not included
PMA	not included

### 3. Experimental configuration and cohort

We included 48 scans from 31 patients of a longitudinal cohort that involves preterm infants from the preterm cohort at Hospital Puerta del Mar (HUPM), Cadiz, Spain, with very low weight at birth, equal or <1,500 grams, and/or gestational age (GA) at birth equal or <32 weeks. The parents or legal guardians of these infants have signed the informed consent. Data were recorded prospectively from these patients as they underwent MRI as part of a cohort study of the preterm brain damage group at the Biomedical research and innovation institute of Cadiz (INIBICA). GA is calculated from the date of the last menstrual period and confirmed using data from early antenatal ultrasound scans. The weeks of postnatal life (age) are added to the weeks of GA at birth, giving the so-called post-menstrual age (PMA). Typically, two MRI scans are taken from each infant. An early scan was performed within the first ten days of life, and a late one was at the term-equivalent age (38–42 weeks of corrected age), according to PMA. Following this principle, the initial 48 MRI scans are divided into two groups, i.e. 23 early scans and 25 term-equivalent scans (17 patients have both scans). In addition, 12 patients are identified as abnormal in agreement with Kidokoro et al. [13]. Therefore, early and term-equivalent scans, plus abnormal/normal MRI scores, provide four different groups: early normal MRI score, early abnormal MRI score, term-equivalent normal MRI score, and term-equivalent abnormal MRI score. Moreover, ten scans from the M-CRIB 2.0 atlas [15] are added to the analyses. These scans are from healthy term-born neonates and are used as the control group.

## 4. Results

### 4.1. Analysis of extracted features

We extracted ten features from the segmented thalamus (see section 2.2). As visualizing all these features are not easy, we rely on the dimension reduction methods such as principal component analysis (PCA). Figure 3 shows the results of PCA on term-equivalent and M-CRIB 2.0 atlas [15] scans. Initial results demonstrate that the first five principal components can explain more than 92% of the variabilities among features. Therefore, these components are enough to explain our data. Table 3 shows the percentage of explained variance for each component. The first two components explain more than 60% of the variation among thalamic features. Moreover, Figure 3, indicates that it is possible to separate the M-CRIB 2.0 atlas scans from those of the preterm infants in our cohort according to the first two components. One of the advantages of PCA is its interpretability. For example, ID 23, highlighted in red, shows an anomaly in its first component with a value less than -0.9. This result suggests that clinicians should check this infant. In addition, according to the Kidokoro assessment score, this ID has an abnormal MRI score.

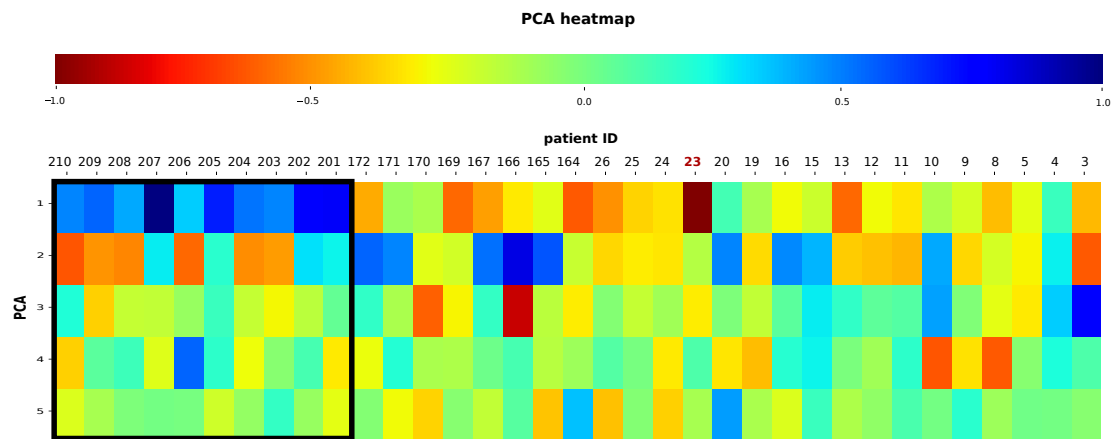


**Figure 3:** Visualising the PCA components of thalamic measurements in preterm infants at term-equivalent age and healthy term-born ones. The horizontal axis of the figure shows the anonymised ID of the patients, and the vertical one shows the number of principal components. The atlas scans IDs start from 201. The box in black colour separates the atlas scans from the rest. Notice that we use 5 components for PCA analysis.

PCA components	1	2	3	4	5
Explained variance	34.7	28.1	13.6	10.5	5.7

**Table 3**

The percentage of variance explained in measurements of thalamic features from different components of PCA.

## 4.2. Clustering results

After clustering, the three clusters are represented by different coloured points and also compared with MRI score [13] (abnormal = green star, normal = magenta cross) and M-CRIB 2.0 atlas [15] (yellow cross) in Figure 4. All the images in the M-CRIB 2.0 atlas [15] are correctly classified in the third cluster. These findings highlight the significant difference between healthy term-born infants and preterm infants at term-equivalent age. Furthermore, Figure 4 also shows that most premature infants with abnormal MRI scores are in the second cluster, i.e. 77%. However, the clustering of thalamic features of the early scan group does not differentiate between abnormal and normal term-equivalent MRI. The second cluster gets the highest probability values for early scans, i.e. 47%. The clustering accuracy is summarized in Table 4.

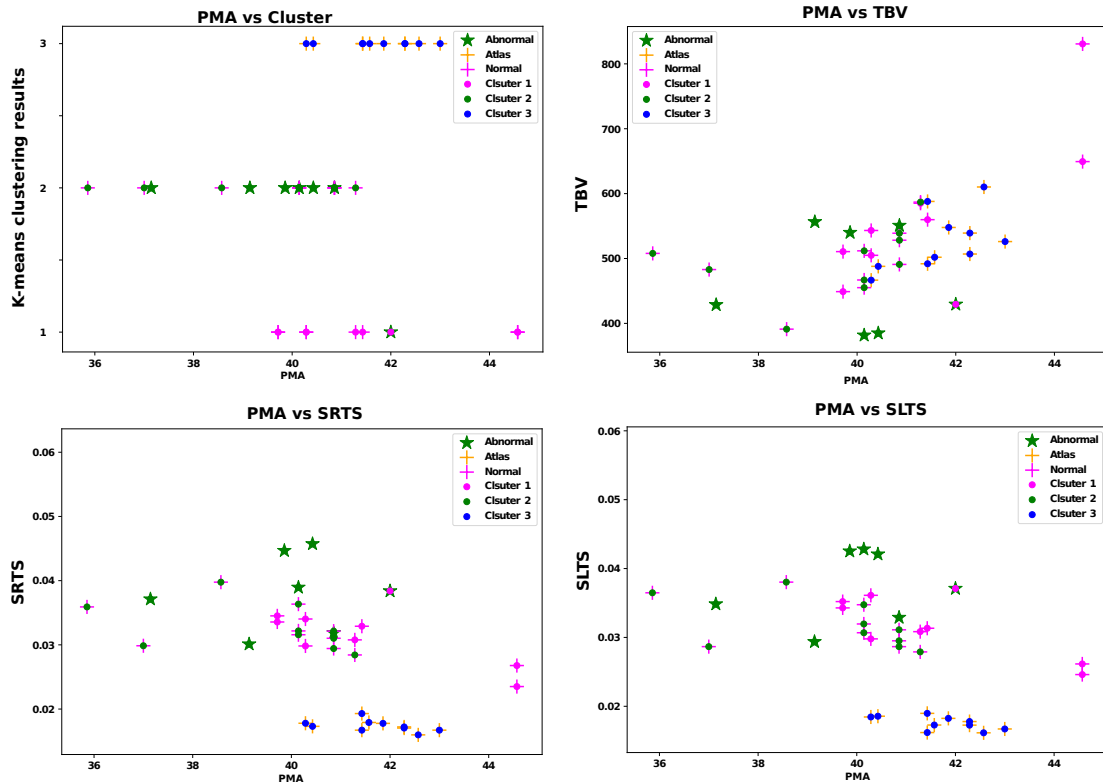


**Figure 4:** The plots of post-menstrual age in weeks (PMA) vs Total Brain Volume in  $\text{cm}^3$  (TBV), Standardised Left Thalamus 3D Surface (SLTS) and Standardised Right Thalamus 3D Surface (SRTS).

**Table 4**

The percentage of abnormal infants in each cluster for the early and term-equivalent scans.

	Cluster 1	Cluster 2	Cluster 3
Early scans	28%	47%	25%
Term-equivalent scans	23%	77%	0%

## 5. Discussion

The K-means clustering correctly separated 77% of abnormal patients into the correct cluster (Table 4) and correctly distinguished all healthy neonates from the M-CRIB 2.0 atlas images, as our reference group (Figure 4). The separation of the third cluster seems easy as the first and the second component of PCA results (Figure 3) indicate the difference in the thalamic features between healthy term-born infants and preterm infants at term-equivalent age.

Nevertheless, the clustering of thalamic features of the early scans does not differentiate between the abnormal and normal MRI (Table 4). This result could be explained by postnatal brain maturation, as the MRI score system only applies to term-equivalent scans, so the patient's situation can change from one scan to the next. In particular, a patient could have a normal early MRI scan and develop clinical complications that will lead to brain injury and an abnormal term-equivalent MRI. After describing the thalamic features of a cohort of preterm and term-born infants related to GA at birth and PMA at the time of scans, we show how the thalamic features can be associated with clinical MRI scores. Furthermore, they share three clustering patterns: the first cluster can be interpreted as patients with normal MRI score, the second cluster can belong to the abnormal MRI score, and the third cluster can be associated with the M-CRIB 2.0 atlas scans.

Some other groups have done previous research on this topic. For example, Ball et al. [12], Jakab et al. [10] and Menegaux et al. [23] focused on the diffusion-weighted imaging. In contrast, we focus on the T1-weighted images in the current study. Furthermore, our work includes a detailed analysis of the thalamic features, while the work published by Wisnowski et al., [24] Lao et al. [25] and Loh et al. [26] considered only one feature, i.e. thalamic volume. Interestingly, our results align with those from Lao et al. [25], who described the standardised 3D surface as an important thalamic feature. Our study includes a more exhaustive analysis of the thalamic features and extensively extracted 2D parameters, including the thalamic perimeter where the largest thalamic area was found in the axial plane, and 3D information from the thalamus [25]. Moreover, we have normalised the thalamic volume to the TBV and studied the association between the specific morphological characteristics of the thalamus and the Kidokoro score [13] at the term-equivalent MRI.

According to Kostović et al. [19], during the beginning of the third trimester of fetal development, thalamocortical and cortico-cortical afferents migrate to the cortex and finally form their primary connections. The ontogeny of this migration process suggests that these connections grow with different starting times but from the same point. Consequently, the other brain regions grow considerably during this period, and their proportion to the thalamus significantly changes (see figure2). Conclusively, damage in the preterm brain affects thalamus features and their relation with the TBV. In some extreme cases, the atlas-based segmentation includes other structures and overestimates the thalamus and its features. Manual segmentation and the development of advanced machine learning methods can help to solve this problem.

## 6. Conclusion

In the current study, we associated the thalamic features with the MRI score assessment of preterm infants and explored the importance of thalamic features for the clustering of the patients. The standardised thalamic 3D surface can be suggested as a crucial morphological feature to cluster patients. Further studies, including a bigger sample size and external validation, are warranted to investigate the potential role of these thalamic features as a diagnostic and predictive tool of brain injury and long-term neurodevelopmental outcomes in preterm infants.

## Acknowledgments

This study was funded by the PARENT project from the European Union's Horizon 2020 research and innovation program under the Marie Skłodowska-Curie Innovative Training Network 2020. Grant Agreement N 956394. BJ, SPL and IBF acknowledge funding from the Cadiz integrated territorial initiative for biomedical research, European Regional Development Fund (ERDF) 2014–2020. Andalusian Ministry of Health and Families, Spain. Registration number: ITI-0019-2019.

## References

- [1] M. Delnord, J. Zeitlin, Epidemiology of late preterm and early term births—an international perspective, in: *Seminars in Fetal and Neonatal Medicine*, volume 24, Elsevier, 2019, pp. 3–10.
- [2] N. Marlow, Outcomes of preterm birth and evidence synthesis, *Developmental Medicine & Child Neurology* 60 (2018) 330.
- [3] A. Pascal, P. Govaert, A. Oostra, G. Naulaers, E. Ortibus, C. Van den Broeck, Neurodevelopmental outcome in very preterm and very-low-birthweight infants born over the past decade: a meta-analytic review, *Developmental Medicine & Child Neurology* 60 (2018) 342–355.
- [4] W. Y. Loh, P. J. Anderson, J. L. Cheong, A. J. Spittle, J. Chen, K. J. Lee, C. Molesworth, T. E. Inder, A. Connelly, L. W. Doyle, et al., Longitudinal growth of the basal ganglia and thalamus in very preterm children, *Brain imaging and behavior* 14 (2020) 998–1011.
- [5] J. J. Volpe, Brain injury in premature infants: a complex amalgam of destructive and developmental disturbances, *The Lancet Neurology* 8 (2009) 110–124.
- [6] I. Kostović, M. Judaš, The development of the subplate and thalamocortical connections in the human foetal brain, *Acta paediatrica* 99 (2010) 1119–1127.
- [7] H. Toulmin, J. O'Muircheartaigh, S. J. Counsell, S. Falconer, A. Chew, C. F. Beckmann, A. D. Edwards, Functional thalamocortical connectivity at term equivalent age and outcome at 2 years in infants born preterm, *cortex* 135 (2021) 17–29.
- [8] R. Ceschin, J. L. Wisnowski, L. B. Paquette, M. D. Nelson, S. Blüml, A. Panigrahy, Developmental synergy between thalamic structure and interhemispheric connectivity in the visual system of preterm infants, *NeuroImage: Clinical* 8 (2015) 462–472.
- [9] G. Ball, J. P. Boardman, P. Aljabar, A. Pandit, T. Arichi, N. Merchant, D. Rueckert, A. D.

- Edwards, S. J. Counsell, The influence of preterm birth on the developing thalamocortical connectome, *Cortex* 49 (2013) 1711–1721.
- [10] A. Jakab, G. Natalucci, B. Koller, R. Tuura, C. Rügger, C. Hagmann, Mental development is associated with cortical connectivity of the ventral and nonspecific thalamus of preterm newborns, *Brain and behavior* 10 (2020) e01786.
- [11] D. K. Thompson, W. Y. Loh, A. Connelly, J. L. Cheong, A. J. Spittle, J. Chen, C. E. Kelly, T. E. Inder, L. W. Doyle, P. J. Anderson, Basal ganglia and thalamic tract connectivity in very preterm and full-term children; associations with 7-year neurodevelopment, *Pediatric Research* 87 (2020) 48–56.
- [12] G. Ball, J. P. Boardman, D. Rueckert, P. Aljabar, T. Arichi, N. Merchant, I. S. Gousias, A. D. Edwards, S. J. Counsell, The effect of preterm birth on thalamic and cortical development, *Cerebral cortex* 22 (2012) 1016–1024.
- [13] H. Kidokoro, J. J. Neil, T. E. Inder, New mr imaging assessment tool to define brain abnormalities in very preterm infants at term, *American Journal of Neuroradiology* 34 (2013) 2208–2214.
- [14] A. Makropoulos, E. C. Robinson, A. Schuh, R. Wright, S. Fitzgibbon, J. Bozek, S. J. Counsell, J. Steinweg, K. Vecchiato, J. Passerat-Palmbach, et al., The developing human connectome project: A minimal processing pipeline for neonatal cortical surface reconstruction, *Neuroimage* 173 (2018) 88–112.
- [15] B. Alexander, W. Y. Loh, L. G. Matthews, A. L. Murray, C. Adamson, R. Beare, J. Chen, C. E. Kelly, P. J. Anderson, L. W. Doyle, et al., Desikan-killiany-tourville atlas compatible version of m-crib neonatal parcellated whole brain atlas: the m-crib 2.0, *Frontiers in Neuroscience* 13 (2019) 34.
- [16] A. Makropoulos, I. S. Gousias, C. Ledig, P. Aljabar, A. Serag, J. V. Hajnal, A. D. Edwards, S. J. Counsell, D. Rueckert, Automatic whole brain mri segmentation of the developing neonatal brain, *IEEE transactions on medical imaging* 33 (2014) 1818–1831.
- [17] G. Li, L. Wang, P.-T. Yap, F. Wang, Z. Wu, Y. Meng, P. Dong, J. Kim, F. Shi, I. Rekik, et al., Computational neuroanatomy of baby brains: A review, *NeuroImage* 185 (2019) 906–925.
- [18] I. Grigorescu, L. Vanes, A. Uus, D. Batalle, L. Cordero-Grande, C. Nosarti, A. D. Edwards, J. V. Hajnal, M. Modat, M. Deprez, Harmonized segmentation of neonatal brain mri, *Frontiers in Neuroscience* 15 (2021) 662005.
- [19] I. Kostović, N. Jovanov-Milošević, The development of cerebral connections during the first 20–45 weeks’ gestation, in: *seminars in fetal and neonatal medicine*, volume 11, Elsevier, 2006, pp. 415–422.
- [20] I. Benavente-Fernández, P. Lubián-López, M. Zuazo-Ojeda, G. Jiménez-Gómez, A. Lechuga-Sancho, Safety of magnetic resonance imaging in preterm infants, *Acta Paediatrica* 99 (2010) 850–853.
- [21] M. L. Gutiérrez, I. B. Fernández, A. Z. Ojeda, S. L. López, Alteraciones en resonancia magnética asociadas a tratamiento con vigabatrina, *Anales de Pediatría: Publicación Oficial de la Asociación Española de Pediatría (AEP)* 96 (2022) 165–166.
- [22] I. Benavente-Fernández, A. García-Cazorla, Y. Jordán-García, A. Capdevila-Cirera, J. Campistol, Diffusion-weighted imaging in pediatric central nervous system infections, *Revista de Neurología* 50 (2010) 133–138.
- [23] A. Menegaux, C. Meng, J. G. Bäuml, M. T. Berndt, D. M. Hedderich, B. Schmitz-Koep,

- S. Schneider, R. Nuttall, J. Zimmermann, M. Daamen, et al., Aberrant cortico-thalamic structural connectivity in premature-born adults, *Cortex* 141 (2021) 347–362.
- [24] J. L. Wisnowski, R. C. Ceschin, S. Y. Choi, V. J. Schmithorst, M. J. Painter, M. D. Nelson, S. Blüml, A. Panigrahy, Reduced thalamic volume in preterm infants is associated with abnormal white matter metabolism independent of injury, *Neuroradiology* 57 (2015) 515–525.
- [25] Y. Lao, Y. Wang, J. Shi, R. Ceschin, M. D. Nelson, A. Panigrahy, N. Leporé, Thalamic alterations in preterm neonates and their relation to ventral striatum disturbances revealed by a combined shape and pose analysis, *Brain Structure and Function* 221 (2016) 487–506.
- [26] W. Y. Loh, P. J. Anderson, J. L. Cheong, A. J. Spittle, J. Chen, K. J. Lee, C. Molesworth, T. E. Inder, A. Connelly, L. W. Doyle, et al., Neonatal basal ganglia and thalamic volumes: very preterm birth and 7-year neurodevelopmental outcomes, *Pediatric research* 82 (2017) 970–978.